



A drone- and field-based investigation of the land degradation and soil erosion at an opencast coal mine dump after 5 years' evolution of natural processes

Wu Xiao^{1,2} · He Ren² · Tao Sui² · Heyu Zhang³ · Yanling Zhao² · Zhenqi Hu²

Received: 18 May 2021 / Accepted: 9 May 2022
© The Author(s) 2022

Abstract

Opencast coal mining has a large impact on the land surface, both at the mining pits themselves and at waste sites. After artificial management is stopped, a reclaimed opencast coal mine dump is affected by wind and water erosion from natural processes, resulting in land degradation and even safety incidents. In this paper, the soil erosion and land degradation after 5 years of such natural processes, at the Xilinhot opencast coal mine dump in Inner Mongolia, were investigated. A multi-source data acquisition method was applied: the vegetation fraction coverage (VFC) was extracted from GF-1 satellite imagery, high-precision terrain characteristics and the location and degree of soil erosion were obtained using a drone, and the physical properties of the topsoil were obtained by field sampling. On this basis, the degree and spatial distribution of erosion cracks were identified, and the causes of soil erosion and land degradation were analyzed using the geographical detector. The results show that (1) multi-source data acquisition method can provide effective basic data for the quantitative evaluation of the ecological environment at dumps, and (2) slope aspect and VFC are the main factors affecting the degree of degradation and soil erosion. Based on above analysis, several countermeasures are proposed to mitigate land degradation: (1) The windward slope be designed to imitate the natural landform. (2) Reasonable engineering measures should be applied at the slope to restrain soil erosion. (3) The Pioneer plants should be widely planted on the platform at the early stage of reclamation.

Keywords Coal mine dump · Ecological restoration · Drone · Soil erosion · Ecosystem stability · Geographical detector

1 Introduction

Coal mining plays an important role in economic development and industrialization progress (Xiao et al. 2020a, b, 2021; Chen et al. 2021; Li et al. 2021). Furthermore, Opencast mining is the most widely used mining method in the world. In the United States, Germany, Australia, Russia and other developed countries, the proportion of

opencast mining reached more than 60%. Although opencast mining has many advantages, such as high safety, high mining efficiency, high recovery rate and low cost (Kennedy 1990), it drastically damages the ecological environment and produces a large amount of coal waste. The dumps formed by the resulting coal waste stack takes up a large area of land, where the surface soil is poor and it is pressed by heavy trucks, resulting in problems for plant roots and an increase in surface runoff. During the rainy season, concentrated precipitation flows into the settlement cracks, causing disasters such as collapse, landslide and debris flow, and seriously threatening the lives of residents nearby (Neugirg et al. 2016). Statistically, the land used for opencast mine dumps accounts for 30%–50% of the total land used for mining. As a large coal mining country, China's coal consumption accounts for 56.8% of its total energy consumption (National Bureau of Statistics, 2020). Also, the proportion of opencast mining production also increase gradually, from about 3.3% in 1998 to about 15%

✉ Zhenqi Hu
huzq1963@163.com

¹ Department of Land Management, Zhejiang University, Hangzhou 310058, China

² Institute of Land Reclamation and Ecological Restoration, China University of Mining and Technology (Beijing), 100083 Beijing, China

³ Guangzhou South China Institute of Natural Resources Science and Technology, Guangzhou 510642, China

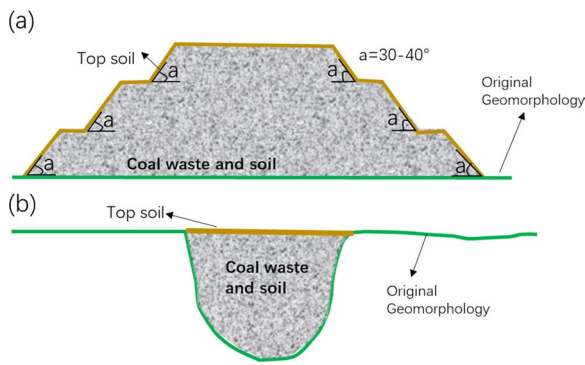


Fig. 1 Concept map of **a** Multi-stage dump, and **b** Gully filled dump

in 2015 (Huang et al. 2015). The average annual additional land area occupied was up to $1 \times 10^4 \text{ hm}^2$ (10^8 m^2), and the soil erosion area increased annually by $3 \times 10^3 \text{ hm}^2$. Therefore, it is important to take account of the safety and stability of the dump when assessing the production safety and economic benefits of the opencast mining areas. The monitoring and maintenance of the dump has become an important aspect of the reclamation process of the opencast mining areas.

The dump is mainly composed of waste material from opencast mining. After the dump reaches its full capacity, it is covered with a layer of topsoil to ensure a rapid restoration of vegetation. The construction of the dump needs to be adapted to local conditions, and the appropriate disposal method should be selected according to the geomorphologic characteristics of the mining area. Several types can be distinguished, such as conical shape, board shape, terrace shape, slope shape, ridge shape, straight shape, or form of flat coverings (Zástěrová et al. 2015). Because of the high cost of land acquisition in China, flat coverings are rarely used. The terraced landform of the Loess plateau can be imitated by designing terraced dumps with a relative height difference of 100–150 m between the platform and the slope intersects (Fig. 1a). Alternatively, fly ash and gangue can be used to carry out a mixed ecological filling of the opencast mine and gully regions in hill (Fig. 1b), laying a foundation for subsequent ecological restoration (Shanxi provincial bureau of quality and technical supervision 2016). However, in the eastern mining areas of northern China, the terrain is flat and topsoil is insufficient. Therefore, most coal waste dumps adopt a multi-stage distribution to reduce the amount of land they occupy.

In view of a series of environmental and safety problems caused by opencast mining, the land reclamation in mining areas has been carried out in many countries. However, in order to restore the ecological system to a stable condition as soon as possible, post-restoration monitoring is still needed. The monitoring mainly includes vegetation restoration, soil

quality and soil erosion. Vegetation restoration is the key to the restoration of dump sites. Vegetation restoration can make full use of the function of the soil-plant composite system, improve the local environment and promote a regional ecological balance, and also significantly improve the soil properties (Wang et al. 2016; Bi et al. 2021). The ideal procedure is to gradually strengthen the composition, structure and level of vegetation, and improve the function of the soil and its water conservation, then finally to achieve self-balance and to establish a stable ecosystem (Wang et al. 2014). At present, in order to improve the success and greening rate of reclamation over a short period of time, most of dump sites were under artificial management. Although a large area of vegetation coverage can be achieved, it is difficult to achieve a state of self-balance in a short time (Ren et al. 2021). Therefore, the monitoring of vegetation degradation and soil erosion of typical dumps under natural conditions can improve the reclamation method and help dumps to reach ecological balance more quickly. However, there is a lack of research on ecological and disaster monitoring of the development of dumps under natural conditions (i.e., without artificial management and protection).

The vegetation fraction coverage (VFC) can quantify the vegetation growth status, serving as an important reference for soil erosion. Besides, the quality of the overlying soil layer affects the restoration of vegetation at the dump (Khalil et al. 2014). The pore structure of the soil affects its hydraulic properties and associated water flow (Wang et al. 2014; Bao et al. 2017). The amount of soil organic carbon (SOC) (Fettweis et al. 2005; Yuan et al. 2018; Zhao et al. 2013), nitrogen (N), phosphorus (P) (Liu et al. 2017) and potassium (K) (Zhou et al. 2017) present in the soil are major determining factors and indicators of its fertility and quality, which are closely related to vegetation restoration. Heavy metals in a soil not only affect plant development but also threaten the health of the surrounding inhabitants through the food chain (Zhao et al. 2010). Vegetation drought resistance (Zhao et al. 2008) and water and soil conservation (Scorpio et al. 2018) can reduce soil erosion. Nevertheless, the high precipitation intensity (Neugirg et al. 2016) in the rainy season causes the soil moisture to reach saturation, and plants and top soil can easily be carried away due to heavy rainfall (Sahle et al. 2019). Inhomogeneous sedimentation (Tomás et al. 2014), and the gradient and aspect (Nyssen and Vermeersch 2010) of the dump slope also have an important effect on soil erosion. Erosion gullies and surface collapses caused by soil erosion led to landslide, debris flow and other disasters, so it is very important to monitor soil quality, vegetation and soil erosion at the dump. Traditional monitoring method is field measurement (Duque et al. 2015; Nyssen et al. 2006b). With the development of geomechanics, some experts began to use mechanical models to estimate the development of soil erosion. Considering the natural factors affecting soil

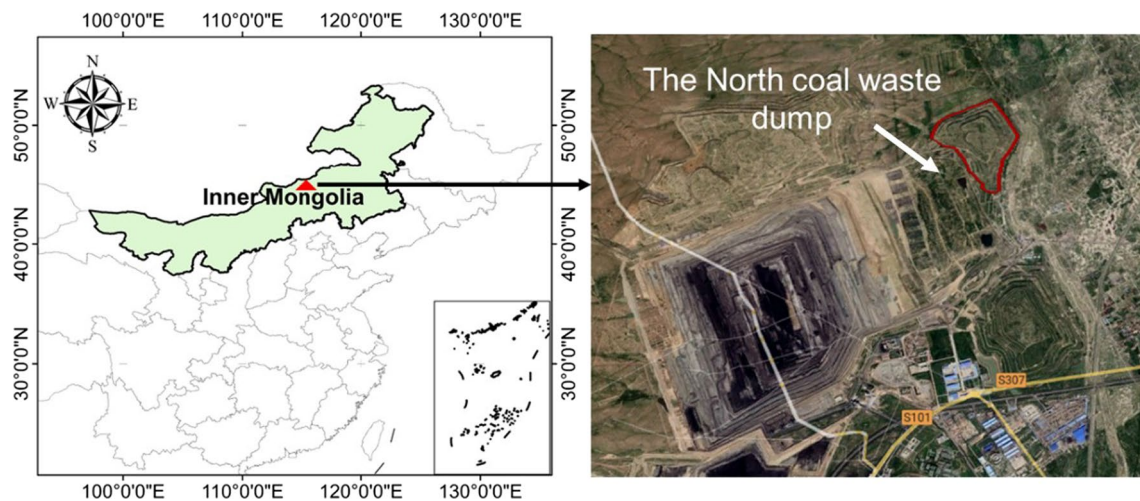


Fig. 2 Location of the study area

erosion, some scholars use the soil erosion equation to conduct quantitative research on soil erosion (Wischmeier and Smith 1978). At present, satellite and drone remote sensing have been widely used in mining areas (Ren et al. 2019; Shahmoradi et al. 2020), which makes multi-frequency and high spatial resolution monitoring possible. Combined with field survey, they were widely used in determination of land deformation (Ćwiąkała et al. 2020; Gong et al. 2021), soil erosion survey (Carabassa et al. 2021), and coal fires monitoring (Yuan et al. 2021) in mining areas.

However, there is a lack of systematic research on the evolution and the associated degradation mechanisms of a coal waste dump under the influence of multiple factors. The causes of water and wind erosion are closely related to the environmental factors, like topography, vegetation information and soil properties. Therefore, it was necessary to analyze the relationship between these environmental factors based on spatial stratified heterogeneity, combining with multi-source data. Aiming this issue, this manuscript was organized as follows: In the second section, an overview of the study area was introduced. In the third section, a research framework was constructed, including the acquisition of accurate topography and field data, the VFC calculation of the coal waste dump, and the soil samples properties. In the fourth section, the importance of different soil erosion factors was assessed by using geographical detector. And the discussion and suggestions were put forward to alleviate the soil erosion of the coal waste dump in the Fifth section. Our research result aims to provide a reference for land reclamation of coal waste dumps in opencast mining areas.

2 Study area

The experimental plot is located at the Western One site of the Shengli coal field, with geographic coordinates of $115^{\circ} 58' - 116^{\circ} 2' 50''$ E, $43^{\circ} 59' - 44^{\circ} 2' 15''$ N, located in Xilinhot, Inner Mongolia Autonomous Region, which is the largest prairie area in China (Fig. 2). The mining area has a typical temperate, semi-arid, continental monsoon climate, where the annual average temperature is 0.3°C and the average wind speed is above 8.5 m/s . The total annual precipitation averages 294.9 mm , with more than 70% occurring from June to August. The average annual effective evaporation is 1811.3 mm , which is more than six times greater than the amount of precipitation. The coal mine has a coal-bearing area of 342 km^2 , with proven reserves of 15.932 billion tons, most of which are suitable for opencast mining.

There are three main external dumping sites, namely south dump, north dump and side dump. All the three waste dumps had been reclaimed, with a green area of 8.64 km^2 . The specific study area is located in north dump of the Western One site of the Shengli coal mine, with an area of 1.07 km^2 (Fig. 2). The dump is divided into four platforms with an altitude range of $980 - 1040\text{ m}$ and a slope angle of 33° . North dump has been reclaimed since 2006, with a total land area of 1.01 km^2 , in which the slope greening area is 0.355 km^2 , the platform greening area is 0.655 km^2 , and the green rate is 100%. Since the cessation of artificial conservation in 2013, the vegetation at the dump site has been degraded, and concentrated precipitation in summer has led to soil erosion, which can easily lead to slope erosion, collapse, debris flow and other disasters under the action of gravity.

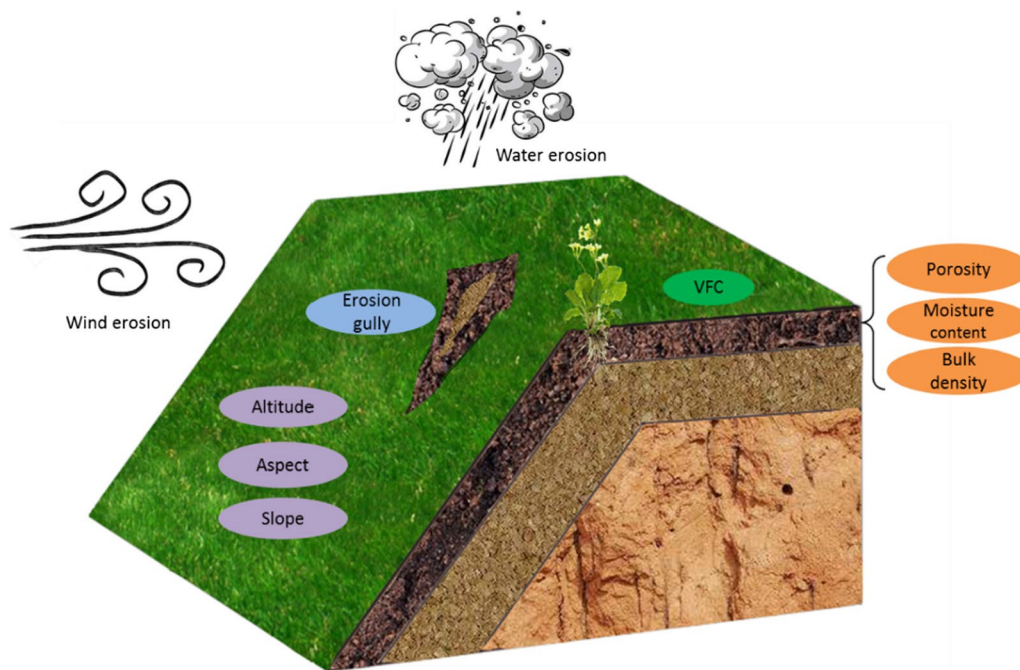


Fig. 3 Potential impact of wind and soil erosion on coal mine dumps under natural conditions

3 Materials and methods

3.1 Framework

As a multi-stage dump, north dump is mainly composed of deep rock-soil, pulverized coal and surface soil close to the coal seam, and siltstone, mudstone and gravel of different sizes away from the stope. The soil is closely packed, with few internal gaps, the permeability coefficient is very small, the seepage storage capacity is very low, and it contains essentially no humus. Without management and protection, dust and soil erosion can easily occur. Therefore, topsoil with a thickness of 30–50 cm has been added to cover the surface. This part of the soil has a high organic matter content and is fully matured. The soil has favorable air permeability, in which the number of seed banks and microorganisms is large, which is conducive to plant growth. After completion of the soil covering and before the arrival of the rainy season, forage grass seeds and shrub seeds with salt-alkali resistance, drought resistance, strong adaptability and nitrogen fixation were planted. Artificial maintenance and management were then carried out for 4 years, including watering, sprinkling and irrigation, adding topdressing fertilizer, disease and insect pest control, soil cultivation and planting. Artificial maintenance and management are quite important for vegetation construction. However, after this was stopped, north dump deformed to different degrees, and its vegetation degenerated, under the influence of wind and rain erosion (Fig. 3). The intense precipitation which occurs

during summer has led to soil and water loss, which can in turn easily lead to erosion ditches, collapse, debris flow and other problems on the slope.

Wind speed and direction in the study area affects wind erosion on the dump, while intense summer precipitation can cause water erosion. In addition to the vegetation cover and topsoil physical properties themselves, the combined action of these factors will jointly lead to degradation of the dump and soil erosion. Obtaining these parameters quantitatively is particularly important. Boggs et al. (2000) used GIS and modeling techniques to assess landform evolution. Hancock et al. (2008) quantified rills on an angle of repose slope of undisturbed mine spoil using a terrestrial laser scanner (TLS). Also, Tarolli and Sofia (2016) analyzed how surface mining affected the environmental landscape using remote sensing technology. However, the interview and modeling methods do not provide complete datasets, while TLS is not suitable for the acquisition of data over a large area, and the visible band of remote sensing is limited by spatial resolution. The research idea of this paper (Fig. 4) is to use a combination of methods to assess the soil erosion and land degradation. The VFC of the dump is calculated using the GF-1 satellite imagery. High precision topographic feature information and the abrasion degree of soil erosion furrows of the dump, in its unmanaged natural state, is done using aerial photogrammetry from a drone equipped with a visible light camera. The physical properties of the topsoil are obtained by interpolation after field sampling. Finally, by analyzing the topsoil physical properties, VFC, elevation,

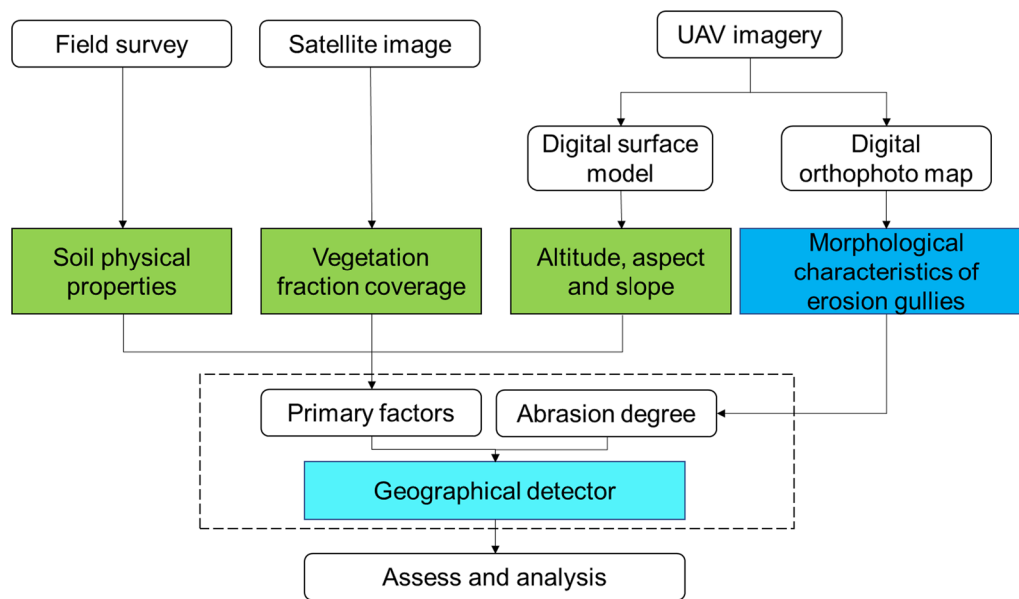


Fig. 4 Methodology flow chart in this study

step slope gradient, slope aspect, and morphological characteristics of erosion gullies in north dump using the geographical detector, the main factors leading to erosion can be identified, providing an effective reference for ecological recovery of the dump in the future.

3.2 Soil properties

Soil is the foundation of vegetation restoration in dump lands, and determines the quality of reclamation (Liu et al. 2016). The physical properties of the soil, such as its moisture content, bulk density, specific gravity, porosity, etc., can influence respiration and the water absorption of plant roots. Soils with deep root systems are characterized by high porosity, high soil infiltration and low soil bulk density (Wang et al. 2018). Nevertheless, the soils of overburden dumps are physically poor, and usually consist of a mixture of coarse-grained particles and rock fragments. In addition, the intensive traffic of heavy machinery used during reclamation can seriously compact soils, further degrading its physical quality. This anthropogenic activity has a significant influence on the soil stability to surface weathering, groundwater or infiltration, gully erosion and slope morphology (Huang et al. 2015).

The physical properties of the topsoil of north dump were obtained by field sampling. Samples from 117 sampling sites were collected in May 2017, uniformly spaced along the dump with a step length of 100 m. The sampling points were supplemented at soil erosion locations (Fig. 5) and the sampling depth was 15 cm. Samples at each sampling point were taken using a cutting ring, placed in a sealed bag, fresh weight of soil

was measured on site, and sent to the laboratory 4 days later to measure their physical properties, including dry weight, porosity, water content and bulk density. The soil moisture content was determined using a drying method. Fresh weight of soil was measured on site, and dry weight was measured after drying in the laboratory. The soil bulk density and total porosity were determined using a cutting ring method. We pressed the ring knife vertically into the topsoil, and dig the ring knife out of the soil with a shovel and flatten the upper and lower ends. Then the soil inside the ring cutter was transferred into the aluminum box without damage and brought back to the laboratory for weighing.

3.3 Vegetation fractional coverage

VFC is calculated from GF-1 remote sensing satellite images, taken in August 2017. The GF-1 satellite is the first satellite of China's high-resolution Earth observation system, launched from the CZ-2D carrier rocket at 12:13:04 on April 26, 2013. It is characterized by the addition of a multispectral camera with high spatial and temporal resolution (Table 1). It is widely used in the fields of geographical mapping, oceanic and atmospheric meteorological observation, water conservation and forestry resources monitoring, fine management of urban areas and transportation, epidemic situation assessment and public health emergency response, and scientific research on the Earth system. Based on the growth cycle of plants and the visibility of satellite images, the multi-spectral image with a spatial resolution of 8 m obtained by GF-1 on August 11, 2016 was adopted. At this time, the plant growth condition was relatively good and there was relatively little cloud cover.

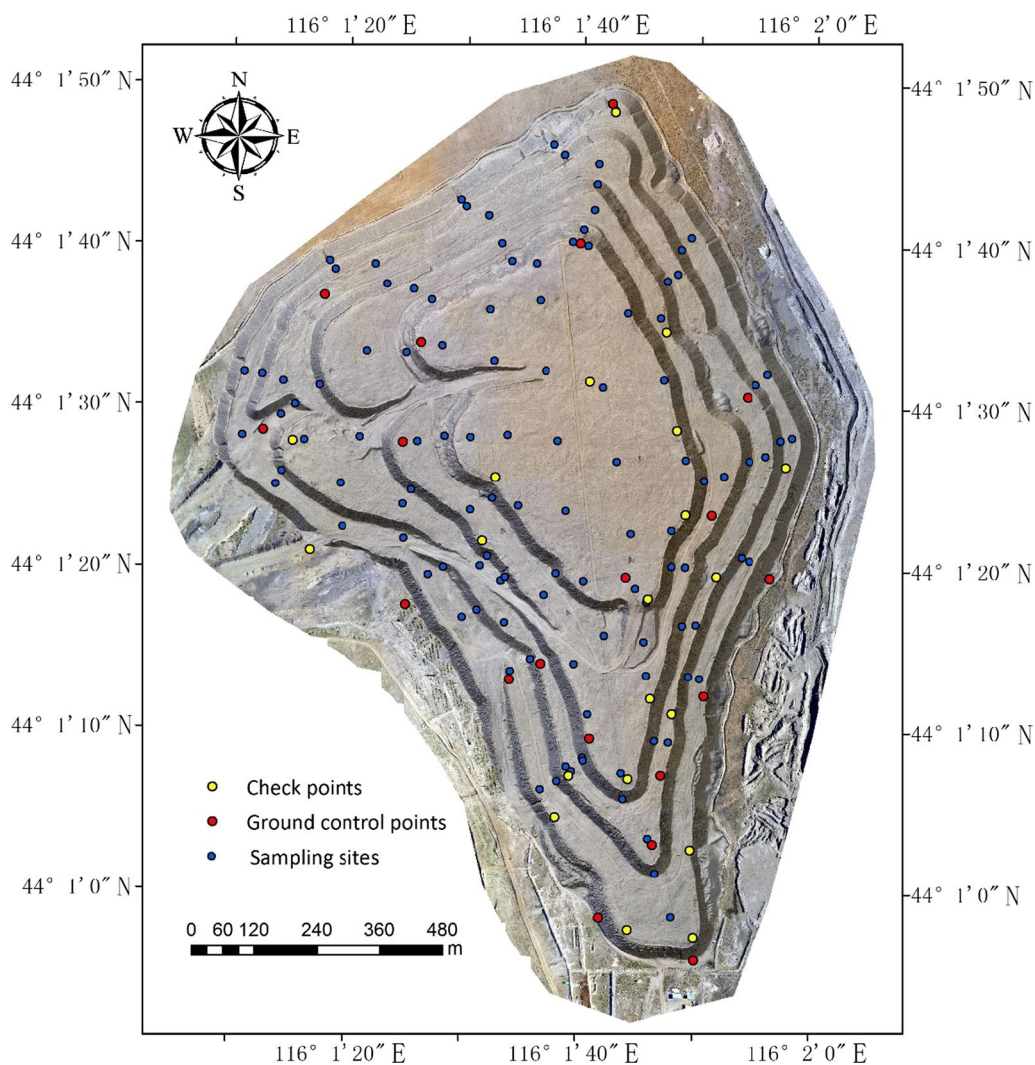


Fig. 5 Sketch map of ground control points, check points and sampling sites

Table 1 Specifications of the GF-1 imagery

Specifications	Details
Orbit type	Sun synchronous and repeating ground trace
Orbit altitude	645 km
Orbit inclination	98.0506°
Descending node local time	10:30 AM
Regression cycle	41 d
Spatial resolution	2 m (Panchromatic camera) 8 m & 16 m (Multispectral camera)
Revisit time	4 d

The study area is located in arid grassland and vegetation is sparse, where few areas have vegetation coverage of more than 90%. Therefore, it is very suitable to take this model estimate the vegetation cover of the dump. Firstly, the normalized difference vegetation index (NDVI) is calculated from the red (*R*) and near infrared (*NIR*) bands of remote sensing images:

To improve the quality and reduce the effects of terrain and atmospheric noise, the images were preprocessed using geometric correction, radiometric calibration, and atmospheric correction from ENVI5.2 software.

$$NDVI = \frac{NIR - R}{NIR + R} \tag{1}$$

where *NIR* and *R* are the 4th and 3rd band of GF-1 satellite imagery, respectively.

VFC is then defined as a uniform NDVI value:

$$VFC = \frac{NDVI - NDVI_S}{NDVI_V - NDVI_S} \tag{2}$$

where *NDVI_S* is NDVI values of bare soil or areas covered with no vegetation; *NDVI_V* is NDVI values of pixels completely covered by vegetation.

These quantities can be calculated from:

$$\text{NDVI}_S = \frac{\text{VFC}_{\max} \cdot \text{NDVI}_{\min} - \text{VFC}_{\min} \cdot \text{NDVI}_{\max}}{\text{VFC}_{\max} - \text{VFC}_{\min}}, \quad (3)$$

$$\text{NDVI}_V = \frac{(1 - \text{VFC}_{\min}) \cdot \text{NDVI}_{\max} - (1 - \text{VFC}_{\max}) \cdot \text{NDVI}_{\min}}{\text{VFC}_{\max} - \text{VFC}_{\min}}. \quad (4)$$

We take $\text{VFC}_{\max}=1$ and $\text{VFC}_{\min}=0$, respectively, so Eq. (2) can be expressed as:

$$\text{VFC} = \frac{\text{NDVI} - \text{NDVI}_{\min}}{\text{NDVI}_{\max} - \text{NDVI}_{\min}} \quad (5)$$

where NDVI values with accumulative probability of 5% and 95% were taken as NDVI_{\min} and NDVI_{\max} respectively.

VFC values range from 0 to 1, and the following results are found in this study, through field investigation and comparison with remote sensing images. An area with VFC greater than 0.8 is a high VFC area, and the plants are mainly *pinus* (Genus), *ulmus pumila* and *armeniaca sibirica* trees. Between 0.4 and 0.8 represents a medium VFC area, and the vegetation mainly includes shrubs such as *C. korshinskii* and *hippophae rhamnoides*. Lower than 0.4 corresponds to a low VFC area, which is dominated by herbs such as *medicago sativa* and *astragalus adsurgens* and bare land.

3.4 Drone photogrammetry

Traditional methods for geomorphological measurement use total station instrument or Global Navigation Satellite Systems (GNSS). Although the measurement accuracy is high, the data density is low, making it difficult to use for fine measurements (Agüera-Vega et al. 2017). Drone photogrammetry can make use of the advantages of aerial triangulation to make a complete and comprehensive observation of the area of interest, and has high measurement efficiency and low cost, so it is widely used in topographic mapping of opencast mining areas. To ensure the elevation accuracy of the digital surface model (DSM), 39 terrain points were measured using CORS (Continuously Operating Reference Stations) with Trimble R8 GNSS receivers. Of these, 19 points were chosen as check points, and the remaining 20 ground control points (GCPs) served as photogrammetric targets (Fig. 5).

The Matrice100 was chosen as the drone platform used in this study. Its fuselage is made of carbon fiber material, making it flexible and light, with a maximum flight duration of 40 min. It can be expanded flexibly and has the possibility to be further developed by the user. The camera used to acquire the images was the ZenmuseX3. The drone took off from the highest platform at a relative flight altitude of 100 m. The longitudinal overlay of the

photos was 80%, and the lateral overlay was 60%. The survey took 57 min and 815 pictures were captured. The processing of the images was performed using the Pix4D mapper software, which allows the reconstruction of a 3D model from the images by applying Structure from Motion (SfM) algorithms. The SfM is an inexpensive method for extracting the 3D information of a scene from multiple overlapping photographs using bundle procedures (Snavely et al. 2008). Pix4D mapper is highly automated, with easy one-key manipulation. Users only need to input coordinates of GCPs and identify the location of GCPs in the images, and it requires neither professional knowledge to process data and view the results nor further human processing of the drone data to automatically generate the digital evaluation model (DEM) and the digital orthophoto map (DOM). Data results can be converted into other formats for other software. The first step is to input them to the Pix4D desktop to carry out image alignment after adjusting for chromatic aberration, noise, and the white balance of the pictures. We obtained the camera position corresponding to each picture, the internal camera orientation parameters, and the sparse point cloud of the terrain, by using feature identification and feature matching. Based on the quality report results, the relative difference of the project was around 2% between the initial and optimized internal camera parameters and all 815 photos were calibrated. The second step is to import and identify GCPs. The terrain profile, composed of a sparse point cloud, can be seen where the aerotriangulation rays intersect, so that GCPs can be easily identified. The georeferencing results showed that the root mean square error (RMSE) of GCPs was 2.3 cm. In the final step, the dense point cloud, 3D scene reconstruction, post-processing, the DSM and the DOM are produced using a one-key procedure. Finally, the DSM and DOM of 5.95 cm ground sample distance (GSD) were obtained. The GSD was an average computed automatically by the Pix4Dmapper software due to the terrain elevation difference of coal waste dump. In addition, it should be pointed out that the drone mission was performed on May, 2017, the end of spring and early summer. The vegetation coverage was less than 10% in field investigation, so it can be used to extract surface terrain information.

3.5 Geographical detector

The geographical detector model was developed for exploring the relationships between spatial patterns of landscapes and the factors which impact them, by Wang et al. (2010). Its principle is that the spatial distributions of two attributes tend to be similar, if there are spatial relationships or interactions between them. The spatial data do not have to

be stratified in geospatial terms, although the attributes can be stratified. The similarity between two attributes can be represented by the so-called power of determinant ($P_{D,H}$), without requiring many external assumptions or constraints. It is defined as:

$$P_{D,H} = 1 - \frac{\sum_{i=1}^m (n_{D,i} \times \sigma_{D,i}^2)}{n\sigma^2} \quad (6)$$

where $P_{D,H}$ is the power of determinant of the D factor to the abrasion degree (H), n refers to the total number of units in the study area, $n_{D,i}$ is the number of cells in the i th partition in the D factor, σ refers to total standard deviation of the abrasion degree, $\sigma_{D,i}$ refers to standard deviation of the i th partition in the D factor, m refers to the strata of D factor.

The geographical detector model is effective at analyzing the effects of different driving factors on spatial heterogeneity, and it has been applied to research on landscapes (Liang and Yang 2016), the environment (Zhang and Zhao 2018) and animal habitats (Liao et al. 2016). Geographical detector was employed in our study to objectively assign weights to different environment factors affecting soil erosion hazards at the dump. As the dependent variable, soil erosion was described by the erosion area. The area of gully erosion was described by the maximum length multiplied by the maximum width, and the area of sheet erosion was identified manually. The independent variables were the slope gradient, elevation, VFC, degree of porosity, bulk density, soil moisture content and slope aspect for each hazard location. In this way, the main driving factors that affect the amount of soil erosion were assessed. The geographical detector consists of four parts, i.e., the factor detector, interaction detector, risk detector, and ecological detector. We focused on the factor detector and the interaction detector in this study.

4 Results

4.1 Soil properties analysis

The main soil components of the dump are siltstone, mudstone, carbonaceous mudstone and chestnut soil. However, the proportion of chestnut soil is very small, with an average overburden thickness of 30 cm, a sandy soil texture and a humus content between 1.5% and 3.0%. Table 2 shows the physical properties of the soil samples. The average bulk density of the topsoil is as high as 1.51 g/cm³, and the average porosity of the soil is 35.89%. The soil tightness is much higher than that of the soil under natural conditions. The average value of soil moisture content was 3.83%, indicating the topsoil has a poor ability to conserve moisture, therefore it has a low fertility and is not conducive to plant growth, making it susceptible to erosion. The sampling points were

interpolated using the Kriging method to obtain the physical properties (Mendes et al. 2019) of the entire dump (Fig. 6), including soil moisture content, porosity and bulk density. The topmost platform is the most heavily compacted, so that it has the smallest porosity, maximum bulk density and minimum water content.

4.1.1 Porosity

The soil porosity of the dump site in the study area is low around and high in the middle, which may be due to the fact that the top platform has been repeatedly rolled by heavy machinery, resulting in soil hardening and topsoil hardening (Liu et al. 2016). Although dust is reduced to a certain extent, the soil with low porosity reduces the infiltration rate of water, resulting in a large amount of surface water runoff, thus causing soil erosion.

4.1.2 Moisture content

The east and west sides of the dump have the highest water content. The high moisture content on the east side is due to the short illumination time and the low evaporation on sunny slopes. The high moisture content in the west is because there is a lane leading to the top on the platform in the west of the dump. After long-term rolling, the platform in the west is sunken, which plays a certain role in water collection. The low moisture content on the south side is due to sunny slopes (Pan et al. 2017). On the north side, the dry and cold monsoon prevailing in spring and winter takes away a large amount of water from the soil surface, so the soil moisture content is low.

4.1.3 Bulk density

The distribution of soil bulk density on slope surface is affected by vegetation and topography. The moisture, nutrient and air content in soil also change with the slope position. As water flows through the surface, it moves fine particles from the soil to the bottom of the slope. With the rain erosion, some slope will also occur collapse. The soil surface structure from the upper slope to the lower slope tends to change from compact to loosed and porous.

4.2 VFC

Vegetation coverage is affected by the physical properties of the topsoil (Huang et al. 2015), plant species (Liu et al. 2016) and local climate (Brown et al. 1997), and there is significant variation in its spatial distribution. The north dump covered 483,580 m² of low vegetation, 453,704 m² of medium vegetation and 120,188 m² of high vegetation on September 1, 2017. As can be seen from Fig. 7a, the

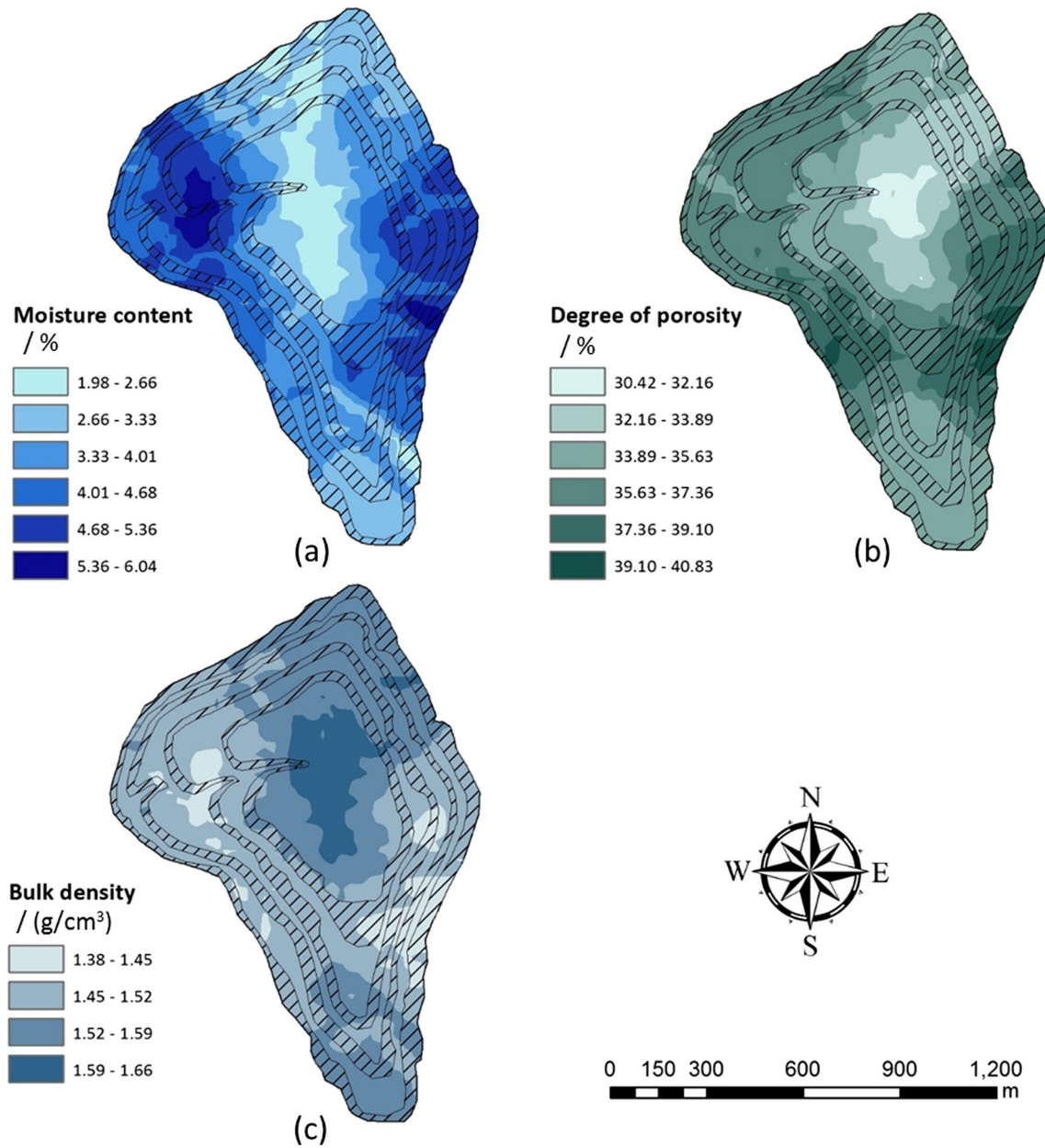


Fig. 6 Map of the soil physical properties. a Moisture content; b Degree of porosity; c Bulk density

Table 2 Soil physical properties measurement

Statistical result	Bulk density (g/cm ³)	Porosity (%)	Moisture content (%)	
			Original value	Logarithmics
Maximum	1.860	55.770	13.298	1.124
Minimum	1.040	21.952	0.667	-0.176
Average	1.511	35.885	3.832	0.498
Median	1.520	35.943	3.019	0.480
Standard deviation	0.150	5.545	2.565	0.270
Variance	0.023	30.746	6.578	0.073

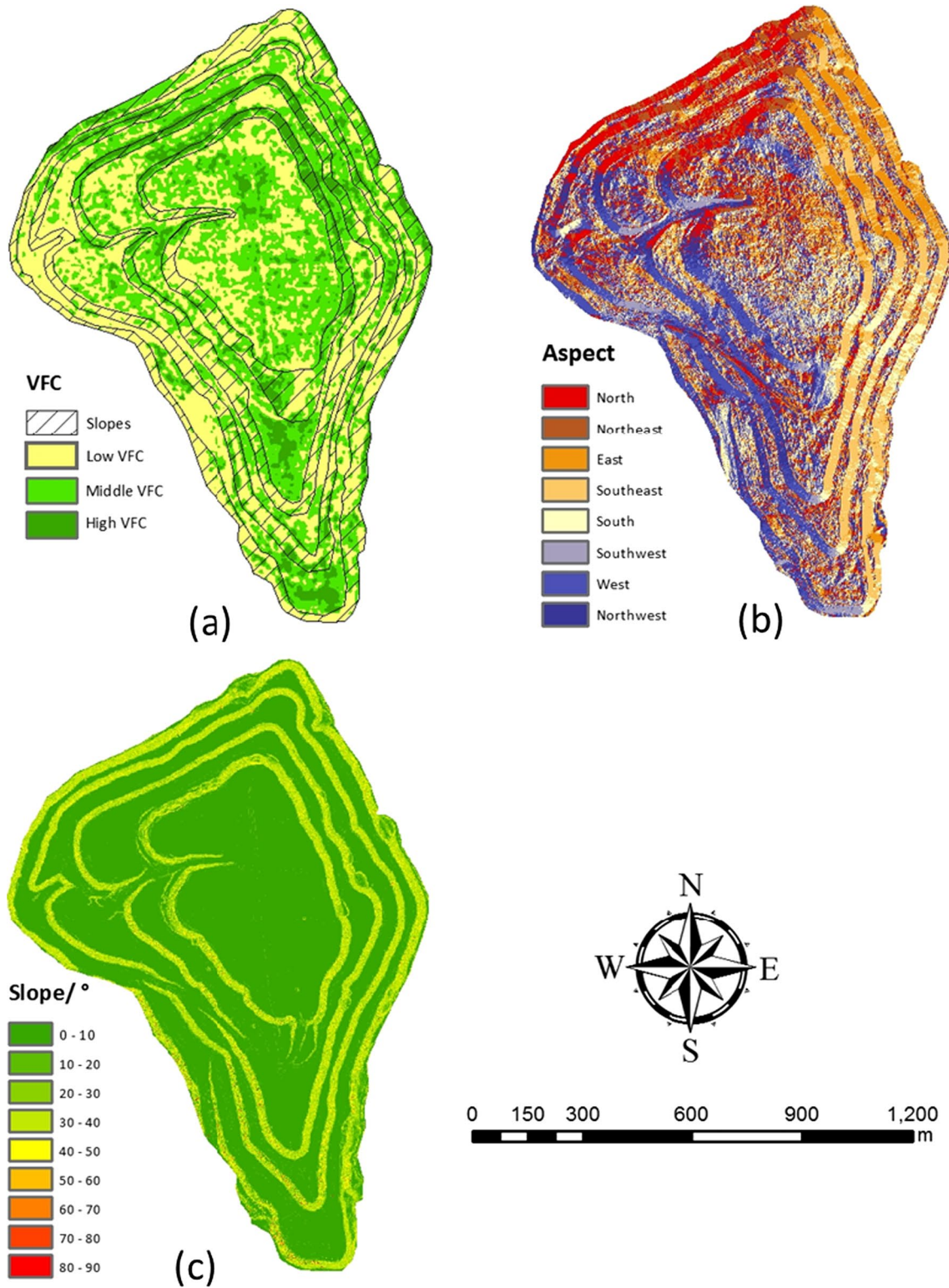


Fig. 7 Map of **a** VFC, **b** Slope aspect and **c** Gradient

high VFC areas are mainly distributed on the slope surface, which has not been compacted by heavy transport equipment and is more conducive to water infiltration and

plant root growth. In the high VFC area of the platform in the south of the dump, because of intensive planting during reclamation, the tree cluster distribution makes

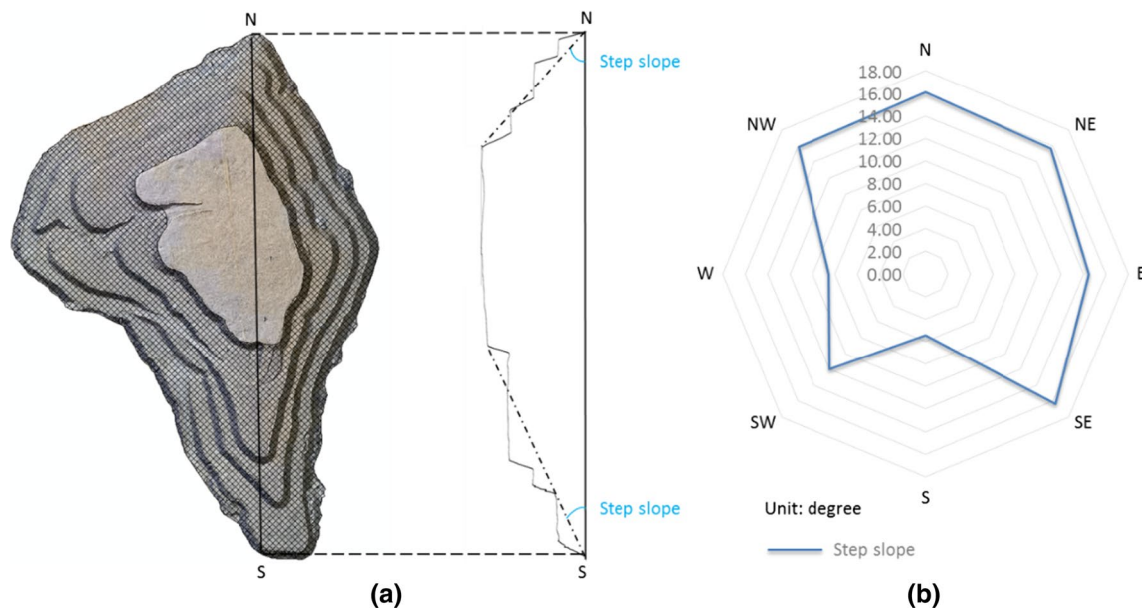


Fig. 8 Step slope. **a** The elevation profile from the DSM is shown on the right, with its location shown on the map on the left. **b** Radar chart of the step's slope gradient

it more stable and not so vulnerable to degradation. In different slope aspect, VFC of north slope and east slope was higher than that of south slope and west slope. It indicates that the growth of vegetation is closely related to the slope direction. The north slope and the east slope are shady slopes with short light time, weak plant transpiration and little water evaporation, while the south slope and the west slope are sunny slopes with long light time, strong plant transpiration and much water evaporation, which is difficult for vegetation restoration.

4.3 Geomorphology and gully erosion

The slope aspect (Fig. 7b) and gradient (Fig. 7c) were then obtained from the DSM. The slope gradients of each platform are approximately equal, at about 33 degrees, however, the step's slope aspects are more variable (Fig. 8). In the north, northwest, northeast, east and southeast directions, the step's slope gradients are about 16 degrees, but in the west, southwest and south directions, the step's slope gradient is significantly shallower, even reaching as low as approximately 6 degrees. The greater the step's slope gradient is, the more vulnerable the surface is to cause Rock fragment movement (Nyssen et al. 2006a) and wind-water erosion (Zhang et al. 2019).

Figure 9 shows the distribution of erosion gullies and collapsed areas. All the geological hazards are located in slope areas. The heavy mechanical equipment used in the dump compacts the dump platform, making it less susceptible to infiltration of heavy rain. However, on the slopes

of the dump, loose rocks and soils, poor stability, and low water content make it vulnerable to water-wind erosion. The erosion gullies radar chart (Fig. 10) shows the erosion extent on four platforms in different directions. It can be found in combination with Table 3, the region with the most serious soil erosion was located west to northwest of the dump, where five collapse areas were concentrated, totaling 7399.57 m², and accounting for 53.72% of the total erosion area. Erosion gullies were mainly distributed on the west side of the dump, accounting for 50% of the total erosion gullies. There were 13 erosion gullies to the west (247.5° to 292.5°), 16 erosion gullies to the northwest (292.5° to 337.5°), and 20 erosion gullies to the southwest (202.5° to 247.5°). The number of erosion gullies on the east side (E, NE, SE) was smaller, accounting for 28.26% of the total. The slope aspect with more severe erosion is in line with the prevailing local wind direction (Nyssen and Vermeersch 2010). The soil erosion of the fourth platform slope(crest) is the most serious, while the soil erosion of the first and second layers is lighter than that of the other two, as also shown by Cha and Tang (2000). This indicates that wind erosion is a significant cause of these hazards.

4.4 Analysis of dump hazards using geographical detector

4.4.1 Factor detector

The factor detector reveals the impact of a single driving factor on the degree of soil erosion. The power of determinant

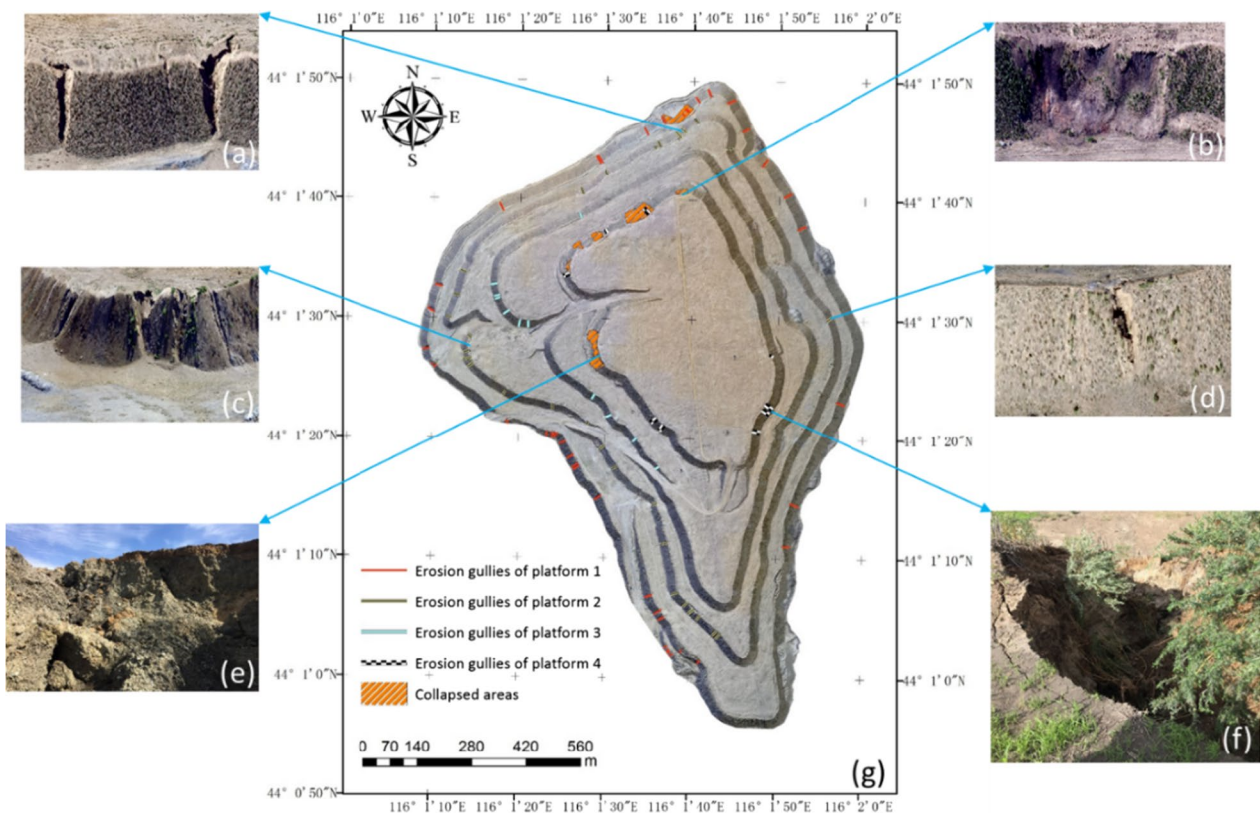


Fig. 9 Geologic hazards at north dump. a–d Hazards shown in 3D models; e–f Photos taken in the field; g Distribution of hazards

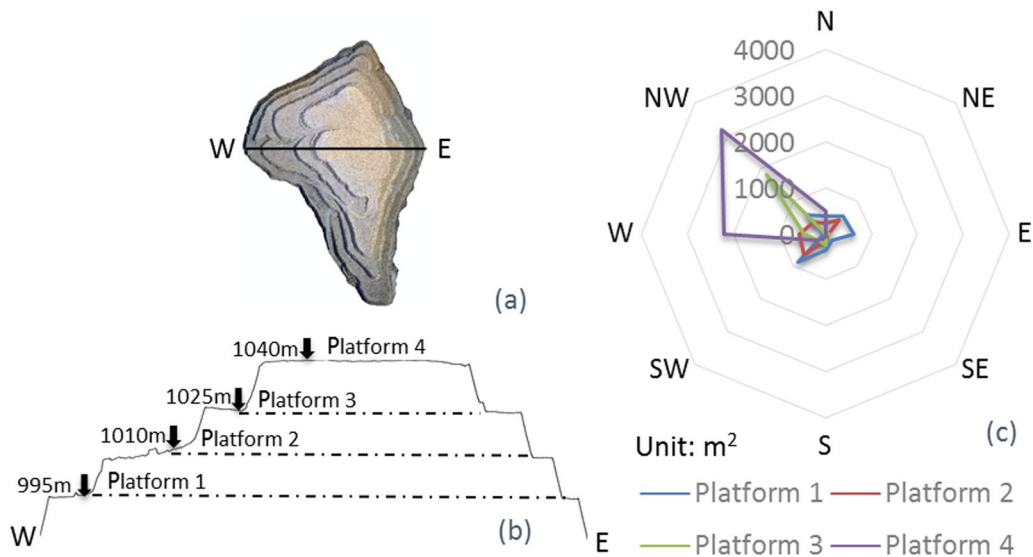


Fig. 10 Erosion gullies radar chart. a Section line; b Transverse section; c Radar chart of erosion extent of each platform. The distance from the center represents the erosion extent

($P_{D,H}$) of each factor is shown in Fig. 11. This shows that the most important contributing factors are elevation (0.127), slope aspect (0.107), and VFC (0.094), followed by step slope gradient (0.051), degree of porosity (0.044),

soil moisture content (0.043), and bulk density (0.028). The larger wind force at the top of the dump accelerates the development of erosion gullies into collapse areas. The collapse areas are mainly concentrated on the slope of the

Table 3 Distribution of soil erosion

Aspect	Erosion gullies	Cumulative gullies ratio (%)	Erosion areas	Cumulative area ratio (%)
N	10	10.87	1108.72	8.79
NE	13	25.00	948.12	16.31
E	8	33.70	747.39	22.23
SE	5	39.13	272.57	24.39
S	10	50.00	827.58	30.95
SW	20	71.74	1933.28	46.28
W	10	82.61	827.58	52.84
NW	16	100.00	5948.07	100.00

fourth platform, indicating that the higher the elevation of an area is, the more vulnerable it is to soil erosion (Zhang et al. 2012). The slope aspect is related to wind direction. The prevailing westerly wind in spring and winter means that erosion gullies are mainly distributed on the west side of the dump. For regions without soil erosion, vegetation can play a role as a wind break and in sand fixation, thus preventing soil erosion. For regions with soil erosion, vegetation can effectively inhibit the development of erosion gullies and prevent the combination of adjacent collapse areas. Gentle topography helps reduce soil erosion, especially on windward slopes, where a smaller gradient slows the acceleration of upwind airflow and gravity subsidence of the topsoil. A surface soil with large porosity is conducive to plant growth and the infiltration of water, thereby reducing water erosion and inhibiting the further development of fissures. The climate in the experimental area is dry. The higher initial soil moisture content is conducive to a stable soil aggregate structure, enhanced soil permeability, and reduced soil disintegration rate, making the soil less susceptible to erosion (Rudolph et al. 1997). The power of determinant $P_{D,H}$ of bulk density is small, indicating that bulk density does not have a large direct impact on soil erosion in the dump.

4.4.2 Interaction detector

Soil erosion on the slope of the dump is the result of the joint action of many environmental factors. In a real environment, the distribution and change of soil erosion cannot be affected by only a single factor or a single natural cause. In order to establish whether any two environment factors influence the degree of soil erosion independently, or interact with each other, the interaction detector is applied. The interactive influence between each pair of driving factors is categorized as follows:

Weaken and nonlinear: $P_{D,H}(x \cap y) < \min(P_{D,H}(x), P_{D,H}(y))$

Weaken and univariate: $\min(P_{D,H}(x), P_{D,H}(y)) < P_{D,H}(x \cap y) < \max(P_{D,H}(x), P_{D,H}(y))$

Enhance and bivariate: $P_{D,H}(x \cap y) > \max(P_{D,H}(x), P_{D,H}(y))$

Independent: $P_{D,H}(x \cap y) = P_{D,H}(x) + P_{D,H}(y)$

Enhance and nonlinear: $P_{D,H}(x \cap y) > P_{D,H}(x) + P_{D,H}(y)$

where x and y are random environment factors in the study area.

This study found that the interaction detectors for abrasion degree can be divided into two types: enhance and bivariate, and enhance and nonlinear. Though the power of determinant of each pair of driving factors was bigger than that of each individual driving factor, there were significant differences in the interaction strength of different factors (Table 4). The interactive effects of the step slope gradient and elevation, soil moisture content and bulk density, and slope aspect and elevation were greater than the maximum of their separate effects. However, the interactive effects of other pairs were greater than the sum of the effects of the corresponding factors individually, indicating a strong synergistic effect between the two factors. The interactive influence power of VFC with other factors is higher than 0.36, indicating that VFC can significantly enhance the impact of various environmental factors on abrasion degree. VFC can be used as an auxiliary indicator factor for the monitoring of the aetiology of erosion and degradation. In addition, driving factor pairs with strong synergistic effects also include: porosity and moisture content, porosity and bulk density, slope aspect and moisture content, and slope aspect and bulk density. The physical properties of the soil are intrinsically related, and the synergistic effect of slope aspect, moisture content and bulk density is mainly reflected in the change of these physical properties caused by wind erosion.

5 Discussions

5.1 Implications

Dumps are inevitable troubles that were formed by opencast mining. Through the analysis in Sect. 4.4, it is concluded that elevation, VFC, and aspect are the main driving factor affecting soil erosion. Soil property and aspect affect the distribution of VFC. VFC, elevation and aspect have combined effects on soil erosion. Slope stability management and soil erosion are worldwide problems (Valkanotis et al. 2018). The temporal and spatial evolution of soil erosion was analyzed by remote sensing (Karan et al. 2016) and model (Wischmeier and Smith 1978; Rodríguez-Caballero et al. 2015). Soil erosion is usually controlled by changing land use patterns (Nearing et al. 2005) and geomorphic

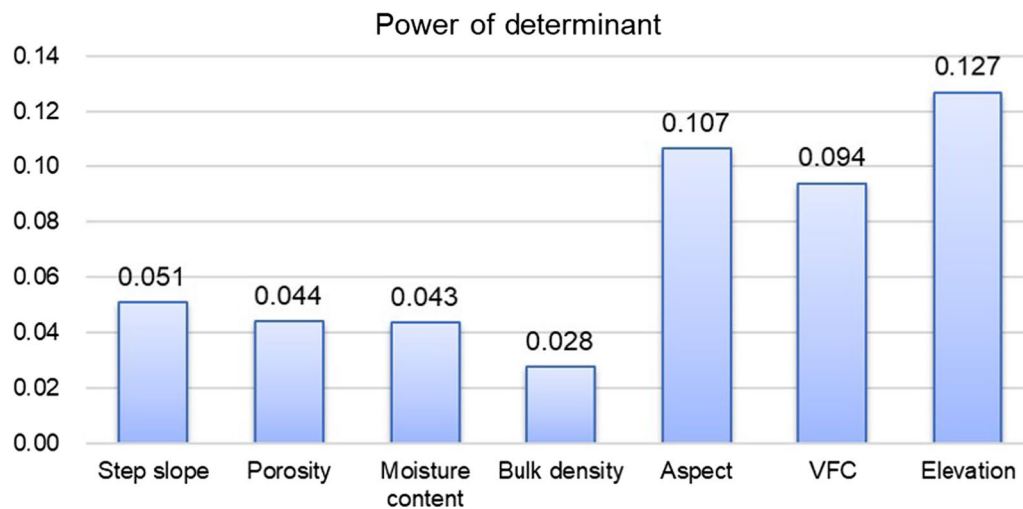


Fig. 11 Influences of different driving factors on the degree of erosion

Table 4 Results of the interaction detector

Item	Step slope gradient	Porosity	Moisture	Bulk density	Slope aspect	VFC	Elevation
Step slope	0.051						
Porosity	0.202	0.044					
Moisture	0.228	0.331	0.043				
Bulk density	0.170	0.481	0.086	0.028			
Slope aspect	0.116	0.243	0.395	0.328	0.107		
VFC	0.443	0.650	0.367	0.399	0.487	0.094	
Elevation	0.194	0.214	0.247	0.206	0.248	0.427	0.127

Values in bold are stronger than other interactions

reclamation. As it was mainly caused by wind erosion and water erosion, the following three suggestions are put forward according to the characteristics of this area:

- (1) Given the serious soil erosion on the windward slope in the west, we suggest reducing the ladder slope gradient to the northwest. The slope would then better reflect the natural landform before its disturbance by human influence, leading to a reduction in wind erosion.
- (2) VFC is not only the main factor affecting soil erosion but also an auxiliary indicator for monitoring soil erosion. Increasing VFC is important for the prevention and treatment of land degradation at dump sites. We can introduce dominant species and appropriately increase the density and diversity of vegetation communities. At the same time, sand barriers and biological arpeggios could be adopted to enhance the stability of vegetation community.
- (3) Strong wind erosion leads to coarser soil surface particles and a great loss of nutrients. Compaction by large

machinery reduces soil porosity and increases bulk density, which is not conducive to plant growth. However, plant roots can reach deep into the soil, promote the agglomeration of micro-aggregates with small particle size, reduce soil bulk density and increase soil porosity, forming a positive feedback loop. Therefore, shrubs and herbaceous pioneer plants with strong adaptability and good survival rates should be widely planted in the early stage of reclamation, so as to provide wind protection, fix the soil and improve the soil structure.

The site-specific suggestions put forward in this paper are applicable to the whole grassland area of Eastern Inner Mongolia. The grassland area of Eastern Inner Mongolia is more than 380,000 km². More than 40 mining areas are scattered in the grasslands of eastern Inner Mongolia. The total coal resources are 249 billion tons, and the annual mining volume is 150–300 million tons. The total area of the dump is more than 14,460 km².

5.2 Limitation of the method and future work

In this paper, a method of soil erosion monitoring based on multi-source data and combined with geographical detector can effectively identify the main factors causing soil erosion, but there are still some scientific problems to be solved. On the one hand, the drone platform can be equipped with multi-spectrum or hyper-spectrum in the future to obtain more spectral information for constructing vegetation parameters. Soil information can be obtained by inverting vegetation parameters, and soil erosion warning can be carried out. On the other hand, using drone loaded RTK can greatly reduce the time of data acquisition, so as to construct a more rapid and efficient monitoring method.

In addition, this thesis only proposes to alleviate wind erosion in the dump by reducing windward slope, but the appropriate gradient is not discussed in depth. In fact, as far back as 1969 geomorphic design approach has been used in landscape planning (McHarg 1969). At present, the geomorphic remodeling of opencast mines in the United States and Australia is mainly based on geomorphic design approach. Common software includes GeoWEPP (Hao et al. 2015), GeoFluv (Hancock et al. 2019), and so on. Because of the high cost of land acquisition in China, mining companies will reduce the land acquisition area as much as possible. How to construct the terrain resistant to wind and water erosion is an important direction of mine restoration in the future.

The combined methodology that integrating satellite remote sensing imagery for vegetation monitoring, drone platforms for accurate terrain and soil erosion investigation, and field sampling for soil property analysis, could fill the gap of different method, that satisfied the demand of coal mine dumps land reclamation monitoring, investigation, assessment.

6 Conclusions

This paper investigates an outer dump at which artificial management has been stopped, as an example to explore the soil erosion after 5 years of evolution of natural processes, and to determine the main factors influencing the degree of soil erosion. The main conclusions are as follows:

- (1) At a height of 100 m, the drone pictures combined with a SfM algorithm can be used to accurately and quickly obtain a 3D model of the dump with a total height of 60 m. The accuracy is sufficient to position and identify the soil erosion area.
- (2) The step's slope gradient of the coal mine dumps is significantly steeper than the natural landform, which

makes the windward slope vulnerable to wind erosion. It is suggested that the windward slope be designed to imitate the natural landform, for example by reducing its gradient.

- (3) Vegetation coverage is the main factor affecting soil erosion. Measures such as sand barriers and biological basketry should be applied at the slope to reduce and restrain gully erosion and planar erosion. Pioneer plants that can improve soil structure should be widely planted on the platform at the early stage of reclamation, so as to facilitate water infiltration and enhance the diversity and stability of vegetation communities during the natural recovery period.
- (4) The combined methodology that integrating satellite remote sensing imagery for vegetation monitoring, drone platforms for accurate terrain and soil erosion investigation, and field sampling for soil property analysis, could fill the gap of different method, that satisfied the demand of coal mine dumps land reclamation monitoring, investigation, assessment.

Acknowledgements This work is supported by the National Key R & D Program of China (Grant No. 2016YFC0501103) and the National Natural Science Foundation of China [Grant No. 420701250].

Declarations

Conflict of interest The authors have declared no conflict of interest.

Open Access This article is licensed under a Creative Commons Attribution 4.0 International License, which permits use, sharing, adaptation, distribution and reproduction in any medium or format, as long as you give appropriate credit to the original author(s) and the source, provide a link to the Creative Commons licence, and indicate if changes were made. The images or other third party material in this article are included in the article's Creative Commons licence, unless indicated otherwise in a credit line to the material. If material is not included in the article's Creative Commons licence and your intended use is not permitted by statutory regulation or exceeds the permitted use, you will need to obtain permission directly from the copyright holder. To view a copy of this licence, visit <http://creativecommons.org/licenses/by/4.0/>.

References

- Agüera-Vega F, Carvajal-Ramírez F, Martínez-Carricondo P (2017) Assessment of photogrammetric mapping accuracy based on variation ground control points number using unmanned aerial vehicle. *Measurement* 98:221–227. <https://doi.org/10.1016/j.measurement.2016.12.002>
- Bao N, Wu L, Ye B et al (2017) Assessing soil organic matter of reclaimed soil from a large surface coal mine using a field spectroradiometer in laboratory. *Geoderma* 288:47–55. <https://doi.org/10.1016/j.geoderma.2016.10.033>
- Bi Y, Xie L, Wang Z et al (2021) Arbuscular mycorrhizal symbiosis facilitates apricot seedling (*Prunus sibirica* L.) growth and

- photosynthesis in northwest China. *Int J Coal Sci Technol* 8(4):473–482. <https://doi.org/10.1007/s40789-021-00408-6>
- Boggs GS, Evans KG, Devonport CC et al (2000) Assessing catchment-wide mining-related impacts on sediment movement in the Swift Creek catchment, Northern Territory, Australia, using GIS and landform-evolution modelling techniques. *J Environ Manag* 59(4):321–334. <https://doi.org/10.1006/jema.2000.0371>
- Brown JH, Valone TJ, Curtin CG (1997) Reorganization of an arid ecosystem in response to recent climate change. *Proc Natl Acad Sci U S A* 94(18):9729–9733. <https://doi.org/10.1073/pnas.94.18.9729>
- Carabassa V, Montero P, Alcañiz JM et al (2021) Soil erosion monitoring in quarry restoration using drones. *Minerals* 11(9):949. <https://doi.org/10.3390/min11090949>
- Cha X, Tang KL (2000) Study on comprehensive control model of small watershed eco-environment in water and wind crisscrossed erosion zone. *J Nat Resour* 15(1):97–100 (in Chinese with English abstract). <https://doi.org/10.11849/zrzyxb.2000.01.017>
- Chen M, Chen X, Hu Z (2021) Contribution of root respiration to total soil respiration during non-growing season in mine reclaimed soil with different covering-soil thicknesses. *Int J Coal Sci Technol* 8(5):1130–1137. <https://doi.org/10.1007/s40789-020-00402-4>
- Ćwiakła P, Gruszczyński W, Stoch T et al (2020) UAV applications for determination of land deformations caused by underground mining. *Remote Sens* 12(11):1733. <https://doi.org/10.3390/rs12111733>
- Duque JFM, Zapico I, Oyarzun R et al (2015) A descriptive and quantitative approach regarding erosion and development of landforms on abandoned mine tailings: new insights and environmental implications from SE Spain. *Geomorphology* 239:1–16. <https://doi.org/10.1016/j.geomorph.2015.02.035>
- Fettweis U, Bens O, Hüttl RF (2005) Accumulation and properties of soil organic carbon at reclaimed sites in the Lusatian lignite mining district afforested with *Pinus* sp. *Geoderma* 129(1–2):81–91. <https://doi.org/10.1016/j.geoderma.2004.12.034>
- Gong C, Lei S, Bian Z et al (2021) Using time series InSAR to assess the deformation activity of open-pit mine dump site in severe cold area. *J Soil Sediment* 2021:1–16. <https://doi.org/10.1007/s11368-021-03040-8>
- Hancock GR, Cawter D, Fityus SG et al (2008) The measurement and modelling of rill erosion at angle of repose slopes in mine spoil. *Earth Surf Proc Land* 33(7):1006–1020. <https://doi.org/10.1002/esp.1585>
- Hancock GR, Duque JFM, Willgoose GR (2019) Geomorphic design and modelling at catchment scale for best mine rehabilitation—the Drayton mine example (New South Wales, Australia). *Environ Modell Softw* 114:140–151. <https://doi.org/10.1016/j.envsoft.2018.12.003>
- Hao Y, Yu R, Hao R et al (2015) Research development on geo-spatial interface for water erosion prediction project. *Adv Sci Technol Water Resour.* 3(in Chinese with English abstract) <https://doi.org/10.3880/j.issn.1006-7647.2015.03.019>
- Huang L, Zhang P, Hu Y (2015) Vegetation succession and soil infiltration characteristics under different aged refuse dumps at the Heidaigou opencast coal mine. *Glob Ecol Conserv* 4:255–263. <https://doi.org/10.1016/j.gecco.2015.07.006>
- Karan SK, Samadder SR, Maiti SK (2016) Assessment of the capability of remote sensing and GIS techniques for monitoring reclamation success in coal mine degraded lands. *J Environ Manag* 182:272–283. <https://doi.org/10.1016/j.jenvman.2016.07.070>
- Kennedy BA, Kennedy BA (eds) (1990) *Surface mining*. SME
- Khalil A, Hanich L, Hakkou R et al (2014) GIS-based environmental database for assessing the mine pollution: a case study of an abandoned mine site in Morocco. *J Geochem Explor* 144:468–477. <https://doi.org/10.1016/j.gexplo.2014.03.023>
- Li S, Zhao Y, Xiao W et al (2021) Optimizing ecological security pattern in the coal resource-based city: a case study in Shuozhou City, China. *Ecol Indic* 130:108026. <https://doi.org/10.1016/j.ecolind.2021.108026>
- Liang P, Yang X (2016) Landscape spatial patterns in the Maowusu (Mu Us) Sandy Land, northern China and their impact factors. *CATENA* 145:321–333. <https://doi.org/10.1016/j.catena.2016.06.023>
- Liao Y, Wang X, Zhou J (2016) Suitability assessment and validation of giant panda habitat based on geographical detector. *J Geoinform Sci* 18(6):767–778. <https://doi.org/10.3724/SPJ.1047.2016.00767>
- Liu X, Zhou W, Bai Z (2016) Vegetation coverage change and stability in large open-pit coal mine dumps in China during 1990–2015. *Ecol Eng* 95:447–451. <https://doi.org/10.1016/j.ecoleng.2016.06.051>
- Liu X, Bai Z, Zhou W et al (2017) Changes in soil properties in the soil profile after mining and reclamation in an opencast coal mine on the Loess Plateau, China. *Ecol Eng* 98:228–239. <https://doi.org/10.1016/j.ecoleng.2016.10.078>
- McHarg IL (1969) *Design with nature*. American Museum of Natural History, New York
- Mendes WS, Neto LGM, Demattê JAM et al (2019) Is it possible to map subsurface soil attributes by satellite spectral transfer models? *Geoderma* 343:269–279. <https://doi.org/10.1016/j.geoderma.2019.01.025>
- Nearing MA, Jetten V, Baffaut C et al (2005) Modeling response of soil erosion and runoff to changes in precipitation and cover. *CATENA* 61(2–3):131–154. <https://doi.org/10.1016/j.catena.2005.03.007>
- Neugirg F, Stark M, Kaiser A et al (2016) Erosion processes in calanchi in the Upper Orcia Valley, Southern Tuscany, Italy based on multi-temporal high-resolution terrestrial LiDAR and UAV surveys. *Geomorphology* 269:8–22. <https://doi.org/10.1016/j.geomorph.2016.06.027>
- Nyssen J, Vermeersch D (2010) Slope aspect affects geomorphic dynamics of coal mining spoil heaps in Belgium. *Geomorphology* 123(1–2):109–121. <https://doi.org/10.1016/j.geomorph.2010.07.004>
- Nyssen J, Poesen J, Moeyersons J et al (2006a) Processes and rates of rock fragment displacement on cliffs and scree slopes in an amba landscape, Ethiopia. *Geomorphology* 81(3–4):265–275. <https://doi.org/10.1016/j.geomorph.2006.04.021>
- Nyssen J, Poesen J, Veyret-Picot M et al (2006b) Assessment of gully erosion rates through interviews and measurements: a case study from Northern Ethiopia. *Earth Surf Process Landf* 31(2):167–185. <https://doi.org/10.1002/esp.1317>
- Pan J, Bai Z, Cao Y et al (2017) Influence of soil physical properties and vegetation coverage at different slope aspects in a reclaimed dump. *Environ Sci Pollut Res* 24(30):23953–23965. <https://doi.org/10.1007/s11356-017-9974-5>
- Ren H, Zhao Y, Xiao W et al (2019) A review of UAV monitoring in mining areas: current status and future perspectives. *Int J Coal Sci Technol* 6(3):320–333. <https://doi.org/10.1007/s40789-019-00264-5>
- Ren H, Zhao Y, Xiao W et al (2021) Influence of management on vegetation restoration in coal waste dump after reclamation in semi-arid mining areas: examining ShengLi coalfield in Inner Mongolia, China. *Environ Sci Pollut Res* 28(48):68460–68474. <https://doi.org/10.1007/s11356-021-15361-9>
- Rodríguez-Caballero E, Cantón Y, Jetten V (2015) Biological soil crust effects must be included to accurately model infiltration and erosion in drylands: an example from Tabernas Badlands. *Geomorphology* 241:331–342. <https://doi.org/10.1016/j.geomorph.2015.03.042>
- Rudolph A, Helming K, Diestel H (1997) Effect of antecedent soil water content and rainfall regime on microrelief changes. *Soil Tech* 10(1):69–81. [https://doi.org/10.1016/0933-3630\(95\)00040-2](https://doi.org/10.1016/0933-3630(95)00040-2)

- Sahle M, Saito O, Fürst C et al (2019) Quantifying and mapping of water-related ecosystem services for enhancing the security of the food-water-energy nexus in tropical data-sparse catchment. *Sci Total Environ* 646:573–586. <https://doi.org/10.1016/j.scitotenv.2018.07.347>
- Scorpio V, Crema S, Marra F et al (2018) Basin-scale analysis of the geomorphic effectiveness of flash floods: a study in the northern Apennines (Italy). *Sci Total Environ* 640:337–351. <https://doi.org/10.1016/j.scitotenv.2018.05.252>
- Shahmoradi J, Talebi E, Roghanchi P et al (2020) A comprehensive review of applications of drone technology in the mining industry. *Drones* 4(3):34. <https://doi.org/10.3390/drones4030034>
- Snaveley N, Seitz SM, Szeliski R (2008) Modeling the world from internet photo collections. *Int J Comput Vis* 80(2):189–210. <https://doi.org/10.1007/s11263-007-0107-3>
- Tarolli P, Sofia G (2016) Human topographic signatures and derived geomorphic processes across landscapes. *Geomorphology* 255:140–161. <https://doi.org/10.1016/j.geomorph.2015.12.007>
- Tomás R, Romero R, Mulas J et al (2014) Radar interferometry techniques for the study of ground subsidence phenomena: a review of practical issues through cases in Spain. *Environ Earth Sci* 71(1):163–181. <https://doi.org/10.1007/s12665-013-2422-z>
- Valkaniotis S, Papathanassiou G, Ganas A (2018) Mapping an earthquake-induced landslide based on UAV imagery; case study of the 2015 Okeanos landslide, Lefkada, Greece. *Eng Geol* 245:141–152. <https://doi.org/10.1016/j.enggeo.2018.08.010>
- Wang J, Li X, Christakos G et al (2010) Geographical detectors-based health risk assessment and its application in the neural tube defects study of the Heshun Region, China. *Int J Geogr Inf Sci* 24(1):107–127. <https://doi.org/10.1080/13658810802443457>
- Wang J, Zhang M, Bai Z et al (2014) Multi-fractal characteristics of reconstructed soil particle in opencast coal mine dump in loess area. *Trans Chin Soc Agric Eng* 30(4):230–238 (in Chinese with English abstract). <https://doi.org/10.3969/j.issn.1002-6819.2014.04.028>
- Wang J, Wang H, Cao Y et al (2016) Effects of soil and topographic factors on vegetation restoration in opencast coal mine dumps located in a loess area. *Sci Rep* 6(1):1–11. <https://doi.org/10.1038/srep22058>
- Wang J, Lu X, Feng Y et al (2018) Integrating multi-fractal theory and geo-statistics method to characterize the spatial variability of particle size distribution of minesoils. *Geoderma* 317:39–46. <https://doi.org/10.1016/j.geoderma.2017.12.027>
- Wischmeier WH, Smith DD (1978) Predicting rainfall erosion losses: a guide to conservation planning. Department of Agriculture, Science and Education Administration
- Xiao W, Deng X, He T et al (2020a) Mapping annual land disturbance and reclamation in a surface coal mining region using google earth engine and the landtrendr algorithm: a case study of the shengli coalfield in Inner Mongolia, China. *Remote Sens* 12(10):1612. <https://doi.org/10.3390/rs12101612>
- Xiao W, Zhang W, Ye Y et al (2020b) Is underground coal mining causing land degradation and significantly damaging ecosystems in semi-arid areas? A study from an Ecological Capital perspective. *Land Degrad Dev* 31(15):1969–1989. <https://doi.org/10.1002/ldr.3570>
- Xiao W, Chen W, Deng X (2021) Coupling and coordination of coal mining intensity and social-ecological resilience in China. *Ecol Indic* 131:108167. <https://doi.org/10.1016/j.ecolind.2021.108167>
- Yuan Y, Zhao Z, Li X et al (2018) Characteristics of labile organic carbon fractions in reclaimed mine soils: evidence from three reclaimed forests in the Pingshuo opencast coal mine, China. *Sci Total Environ* 613:1196–1206. <https://doi.org/10.1016/j.scitotenv.2017.09.170>
- Yuan G, Wang Y, Zhao F et al (2021) Accuracy assessment and scale effect investigation of UAV thermography for underground coal fire surface temperature monitoring. *Int J Appl Earth Obs* 102:102426. <https://doi.org/10.1016/j.jag.2021.102426>
- Zástěrová P, Marschalko M, Niemiec D et al (2015) Analysis of possibilities of reclamation waste dumps after coal mining. *Proced Earth Planet Sci* 15:656–662. <https://doi.org/10.1016/j.proeps.2015.08.077>
- Zhang X, Zhao Y (2018) Identification of the driving factors' influences on regional energy-related carbon emissions in China based on geographical detector method. *Environ Sci Pollut Res* 25(10):9626–9635. <https://doi.org/10.1007/s11356-018-1237-6>
- Zhang Z, Wieland R, Reiche M et al (2012) Identifying sensitive areas to wind erosion in the Xilingele grassland by computational fluid dynamics modelling. *Ecol Inf* 8:37–47. <https://doi.org/10.1016/j.ecoinf.2011.12.002>
- Zhang J, Yang M, Deng X et al (2019) The effects of tillage on sheet erosion on sloping fields in the wind-water erosion crisscross region of the Chinese Loess Plateau. *Soil Tillage Res* 187:235–245. <https://doi.org/10.1016/j.still.2018.12.014>
- Zhao Z, Cai Y, Fu M et al (2008) Response of the soils of different land use types to drought: eco-physiological characteristics of plants grown on the soils by pot experiment. *Ecol Eng* 34(3):215–222. <https://doi.org/10.1016/j.ecoleng.2008.08.003>
- Zhao Z, Xi M, Jiang G et al (2010) Effects of IDSA, EDDS and EDTA on heavy metals accumulation in hydroponically grown maize (*Zea mays* L.). *J Hazard Mater* 181(1–3):455–459. <https://doi.org/10.1016/j.jhazmat.2010.05.032>
- Zhao Z, Shahroui I, Bai Z et al (2013) Soils development in opencast coal mine spoils reclaimed for 1–13 years in the West-Northern Loess Plateau of China. *Eur J Soil Sci* 55:40–46. <https://doi.org/10.1016/j.ejsobi.2012.08.006>
- Zhou W, Yang K, Bai Z et al (2017) The development of topsoil properties under different reclaimed land uses in the Pingshuo opencast coalmine of Loess Plateau of China. *Ecol Eng* 100:237–245. <https://doi.org/10.1016/j.ecoleng.2016.12.028>

Publisher's note Springer Nature remains neutral with regard to jurisdictional claims in published maps and institutional affiliations.